FLOW FIELD ANALYSIS OF STIRRED LIQUID-LIQUID SYSTEMS IN SLIM REACTORS

Sebastian Maaß[1*], Thomas Eppinger[1], Sebastian Altwasser[2], Torsten Rehm[3], Matthias Kraume[1]

[1]Technische Universität Berlin, Straße des 17. Juni 135, Sekr. MA 5-7, 10623 Berlin, Germany

[2]Anhalt University of Applied Sciences, Bernburger Straße 55, 06366 Köthen/Anhalt, Germany

[3]Vinnolit GmbH, 84489 Burghausen, Germany

[*]corresponding author (sebastian.maass@tu-berlin.de)

ABSTRACT

Previous studies showed the great potential but also the great challenges with handling slim reactors often used for polymerization reactions. Experiments and simulations are carried out in reactors with aspect to diameter ratios up to 5 to test and evaluate the mixing and dispersion efficiency for liquid-liquid systems of single and multiple stage impellers. Therefore, power consumption, mixing time and minimum dispersion speed are determined for five different stirrer types under turbulent conditions. It is found that the dimensionless mixing time is highly sensitive to the configuration of the impellers, with almost no dependency on the turbulent power number. Another focus was the analysis of the effect of baffles. The influence of the baffle length in slim reactors on the mixing time and the macroscopic flow field has been determined. An optimal agitation configuration for liquid-liquid systems in slim reactors was determined based on the achieved results: fully baffled multi stage impellers should be used rather than single stage impellers. These impellers save power and allow complete dispersion also for reactors with aspect ratios larger than 3. The first impeller should be installed close to the reactor bottom. The optimum stirrer-stirrer clearance was determined to be two times the stirrer diameter, which is a little larger than the reactor diameters used in this study.

KEYWORDS:

high aspect ratio, baffling effect, liquid-liquid system, Computational Fluid Dynamics, mixing time, minimum dispersion speed

1 INTRODUCTION

Slim liquid-liquid reactors are widely used in process industries, for example, in polymerization reactions like poly vinyl chloride (PVC) production processes. Growing markets and growing economies lead to higher production rates. To achieve this, the reactor size is increased while the reactor diameter is fixed due to space limitations and equipment transportation issues. As a consequence, the ratio of liquid level height H versus reactor diameter T of such apparatus is increased; a ratio of 2.5 or higher is common and values of 5 are expected in

the future. Predictive models for stirred vessels with a reactor height vs. diameter ratio of 1.0 are widely represented in the literature. Since the understanding of dispersion processes in slim reactors is incomplete and differs from the standard system, additionally difficulties are expected. Thus, the scale up of a slim reactor from pilot plant to industrial scale remains a process where much empiricism as well as expensive and time-consuming experimental programs are usually required [1].

Mixing time is a critical parameter for the scale-up, design and operation of agitated reactors. It can be compared with the mass transfer time or reaction time in order to evaluate the determining mechanism of a process. Over the past decades, a lot of research on this subject has been published. Some of them focused on the measurement technique and experiments [2-5], while others achieved empirical correlations from their experimental work [6, 7]. A major emphasis was made on analyzing gas-liquid systems either experimentally or numerically [8, 9]. Jahoda and colleagues have worked for more than a decade on analyzing the homogenization of reactors with high aspect ratios, agitated with multiple impellers [10-13]. Their experiments [10] and simulations [11-13] for multiple Rushton and pitched bladed turbines are an excellent base for understanding the flow field in slim reactors with H/T up to 4.0. Additionally the works of Jaworski et al. are recommended [14]. They are discussing based on several experiments the advantages and limitations of simulations using computational fluid dynamics (CFD) as the computed mixing times were about two to three times longer than the measured values.

Clearly, once multiple impellers are employed, particularly for H/T ratios significantly different from 1.0, the system becomes considerably more complex. Mixing times can significantly increase, and the kind and arrangement of impellers become very important. This study was carried out to determine a highly efficient impeller configuration for slim polymerization reactors. All tested impellers belong to the group of radial flow impellers. This type is commonly used for low to medium viscosity fluids, occurring in polymerization reactions. Although they can be used for any type of single- and multiple-phase mixing duty, they are most effective for liquid–liquid dispersion, compared to axial flow impellers [15]. Radial impellers provide higher shear and turbulence levels with lower pumping volume flows compared to axial impellers. An overview of radial and axial impellers is given by Hemrajani and Tatterson [15].

Mixing, carried out to reduce inhomogeneities in a system, takes place on several scales: macro, meso and micro mixing [16]. The experiments in this research were carried out to analyze the mixing and dispersion behavior of different polymerization reactors on the macro level. The CFD simulations have the same aim.

The work is structured as follows: In chapter two the theoretical background on predicting the mixing time in agitated reactors is given. The experimental set-up, the measurement proce-

dure and the numerical scheme of the CFD simulations used are explained in chapter three. The following results and discussion chapter is separated into two parts. The first part deals with the baffling effect in slim reactors and the second part displays the power number, mixing time and minimum dispersion speed results for various impeller configurations for aspect ratios up to 5.0. The results demonstrate a clear determination for an optimal mixing configuration in slim polymerization reactors.

2 THEORETICAL BACKGROUND

Two main approaches are listed in literature for predicting homogenization of stirred vessels. One is based on bulk flow concepts using either flow numbers or impeller discharge flow rate and power numbers. The other makes use of integral scales of turbulence and their relationship to turbulent diffusion and the decay of concentration gradients [17]. The bulk flow theory assumes full homogenization after 5 circulations for an aspect ratio H/T = 1. Based on that assumption the mixing time θ_{95} is five times the circulation time t_c, which is the quotient from the vessel volume and the pump flow:

$$\theta_{95} = 5 \cdot t_c = 5 \cdot V/\dot{V} \tag{1}$$

Equation (1) can be re-arranged in various ways so that the mixing time shows dependency on power number Ne, vessel diameter T and stirrer diameter D.

The correlations based on the turbulence model first proposed by Corrsin [16, 18] have been extended and further developed by many authors. The basic ideas are very beneficial. Some proposed dependencies from the original equation were questioned by several authors. Nienow [17] was able to predict workgroup independent results, including different impellers with different D/T ratios, power numbers and flow patterns over a very wide range of mean energy dissipation rates ($\varepsilon = P/(\rho V)$) with equation (2).

$$\theta_{95} = 5.9 \cdot T^{2/3} \cdot \varepsilon^{-1/3} (D/T)^{-1/3} = 5.2 \cdot Ne^{-1/3} \cdot (T/D)^2 \cdot n^{-1} \tag{2}$$

Nienow [17] has strongly suggested the use of equation (2) for single impellers in vessels with H/T ratio of 1. The correlation is based on the turbulence theory which does not distinguish between impeller types. Additionally it is in reasonable agreement with many empirical equations [7, 19].

For analyzing the influence of aspect ratios larger than one, the tank diameter T can be replaced [20] by:

$$T = H^{1/4} \cdot T^{3/4} \tag{3}$$

This gives a proportionality of the mixing time on $H^{1/2}$. Grenville and Nienow [20] have mentioned an empirical correlation, which shows a dependency of θ_{95} on $H^{2.43}$:

$$\theta_{95} \cdot n = 3.3 \cdot Ne^{-1/3} (H/D)^{2.43} \quad (4)$$

Fasano and Penney [21] give a more sophisticated, but not universal, correlation with dependency on the impeller geometry by two coefficients C_1 and C_2:

$$\theta_{95} \cdot n = C_1 \cdot (T/D)^{C_2} \cdot (H/T)^{0.5} \quad (5)$$

Five common single stage agitators used for industrial blending operations, two radial and three axial pumping turbines, have been investigated by them. The radial impellers achieved similar values for the constants ($C_1 \cong 3$, $C_2 \cong 2.2$). The empirical constants for the axial impeller are very diverse. The authors noted careful use of the found empirical constants for applying them to other impellers [21]. Nevertheless, this equation is still often used to determine mixing time in slim reactors [22].

Alves et al. [23] propose to model the mixing in slim reactors with multiple impellers by a cascade of well-mixed compartments with backflows. They summarize existing models and compare the number of compartments used per agitator stage. The models examined use from 1 to 4 compartments per agitation stage. The model which consists of 3 compartments per agitation stage is shown to be the best fit to their experimental data [23]. No parameters in that model had to be optimized. Kasat and Pandit [24] are criticizing the conclusion of Alves et al. [23], claiming that the number of compartments used per agitation stage should be one, otherwise this number is an optimization parameter. So they used own experimental results to validate a one compartment per agitation stage model. All their compartments have the same volumes; all impellers are equally distributed over the reactor height (H/T = 3) with a stirrer clearance s = 3·D. One fitting parameter was used to successfully predict the mixing time. The exchange coefficients they used are independent of the Reynolds number in the turbulent regime. The exchange flow rates between the adjacent compartments are 0.34 to 0.44 times the pumping capacity of the impeller configurations used [24].

The influence of the baffling effect on the mixing time was investigated by Lu et al. [6]. They examined the influence of number and width of the baffles with single or triple Rushton turbines. The aspect ratio was always 1. The insertion of the appropriate number of baffles clearly improves the extent of liquid mixing [6]. They correlated the mixing time with the number n_B and the width b of baffles. For a single Rushton turbine the proportionality was: $\theta_{95} \sim b^{-0.16}$. For a triple Rushton turbine the correlation between mixing time and baffle width was $\theta_{95} \sim b^{-0.33}$. Both cases showed a dependency for the number of baffles as follows: $\theta_{95} \sim n_B^{-0.3}$.

Most of the available experimental results have been reproduced with CFD simulations for various numerical boundaries. Ochieng et al. [22] give a compact overview of existing experimental and numerical work on mixing time in stirred tanks. Their comparison of much

data reveals the existence of flow maldistribution caused by system design features. To evaluate the optimal operating conditions with regards to system homogeneity and power consumption, they suggest LES (large eddy simulation) studies with highly refined grids to capture turbulent structures at micro scales.

This overview gives only a small impression of the huge effort by many researchers to analyze and predict stirred applications. The complexity and unknown dependencies between the various influencing parameters still demand explicit and detailed research for the industrial application plants. Therefore detailed experiments and simulations are carried out in this study, to better understand the slim reactors used for the associated polymerization reactions.

3 MATERIAL AND METHODS

3.1 Experimental Set-Up

Four different vessel sizes (T varying from 155 to 990 mm) were used for a wide range of stirrer Reynolds numbers ($Re = nD^2/\nu$). The four different vessels used are described in detail in Figure 1 and Table 1. Two planar baffles were used for all investigations. This is a standard in the example industrial process.

Table 1 – Dimensions of the used stirred tanks and stirrers

	configuration A	configuration B
Geometry parameter	$T_{1,A}$ = 155 mm $T_{2,A}$ = 460 mm	$T_{1,B}$ = 400 mm $T_{2,B}$ = 990 mm
maximum number of used stirrers [-]	four	two
stirrer type	retreat curve impeller (RCI) parallel blade impeller (PBI) crossed blade impeller (CBI)	4 bladed flat blade turbine (4FBT) flat blade paddle impeller (FBI)
b/T	0.08	0.08
D/T	0.55 & 0.60	0.39 & 0.764
h/D	0.25 - 1.65	0.15 & 0.25
H_{max}/T	5.0 2.8	2.5
h_{St}/D	0.06 – 0.24	0.18 - 2.5
s/D	0.1 – 2.5	1.5 – 2.0
l_B/H	0.1 – 1.0 1.0	0.16 – 0.55

Experiments have been performed, using five different radial stirrers. The dimensions are described in detail in Figure 2.The turbulent power numbers $Ne = P/(\rho n^3 D^5)$ are always the

experimentally achieved values for the complete configuration of any multiple impeller system used in this study. The height of the stirrer blades h_{St} is always the sum of the single individuals. So the stirrer height of a dual system is the cumulative height $h_{St} = h_{St,1} + h_{St,2}$. The different configurations have been evaluated for different baffle lengths, liquid level heights and stirrer distances. The results will be presented in the following chapter.

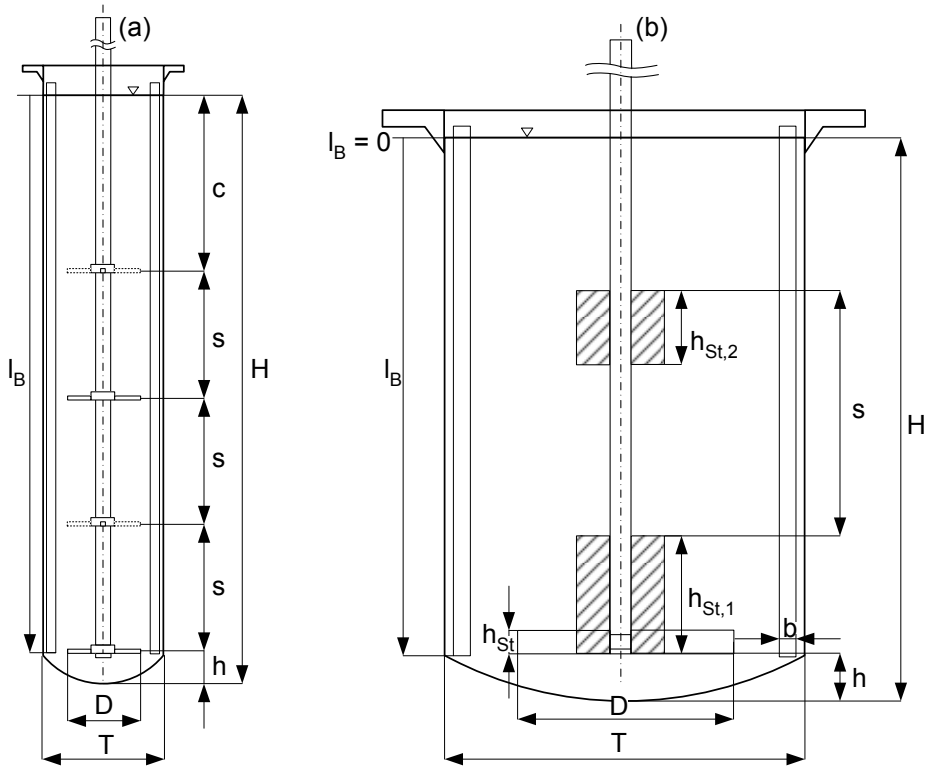

Figure 1 - Experimental set-up and dimensions of the tanks (configuration A – (a); configuration B – (b)) and the stirrers used

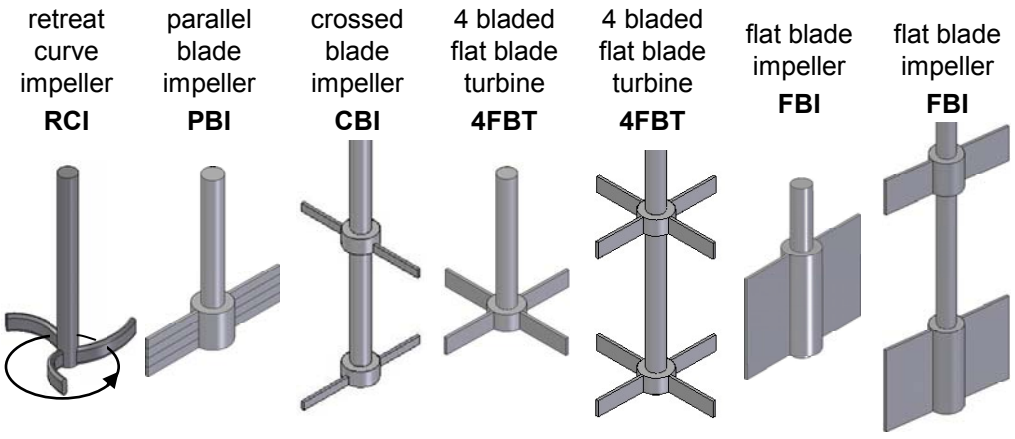

	single stage	single stage	multiple stage	single stage	dual stage	single stage	dual stage
D/T	0.55	0.60	0.60	0.76	0.76	0.39	0.39
h_{St}/D	0.12-0.24	0.06-0.24	0.12-0.24	0.18	0.36	1.57	2.50
s/D	–	–	0.00-3.00	–	1.50	–	2.00
T_1	155 mm	155 mm	155 mm	400 mm	–	400 mm	–
T_2	–	460 mm	460 mm	990 mm	990 mm	990 mm	990 mm

Figure 2 - Design of the radial impellers used

3.2 Measurement Procedure

The measurement technique for the power analysis of each set-up is the same as the one used in previous studies [1]. The stirrers were attached to a viscometer Haake VT 550 to measure the torque and rotational frequency. This procedure is recommended in literature for small scale vessels [25]. It allows the determination of the torque with an accuracy of +/- 100 µNm.

Mixing time measurements were carried out by a decolorization method [26, 27] in which the reactor contents are first colored by alkali and phenolphthalein and subsequently decolorized again by adding a stoichiometric excess of acid. The time from the addition of acid to the disappearance of the last trace of color inside the vessel corresponds to the mixing time and was determined manually. A five percent excess of acid was used which corresponds to a degree of mixing of 95 percent. This value is called the 95% mixing time θ_{95} and is given in equation (6). Upon the conclusion of each mixing time measurement, the actual excess was determined precisely by titration in order to allow a correction [26] to compensate the influence of any possible deviation in concentration. This correction shows the deviation between the desired and the actual stoichiometric excess ($0.05/\delta$ - see equation (6)).

Since the addition site exerts a marked influence on mixing time, the acid was always fed at the same point on the liquid. All experiments were carried out five times with resulting standard deviations always lower than four percent. To achieve comparability with other vessels, the dimensionless mixing time N_θ was calculated based on the stirrer speed n and the 95% mixing time θ_{95}:

$$N_\theta = n \cdot \theta_{95} = n \cdot \frac{\theta_{1-\delta}}{1 + 0.56 \cdot \log\left(\frac{0.05}{\delta}\right)} \tag{6}$$

All mixing time experiments were carried out three times. The deviations between the three trials were always less then 2 percent and hence, were highly reproducible.

In addition the stirrer speed required for complete dispersion, also called minimum impeller speed or minimum dispersion speed n_{min}, was determined also visually. Measurements of this parameter are fraught with difficulty and it is extremely hard to relate published results with one another [28, 29]. This is due to the large difference between "just dispersed," where no continuous layer of the dispersed phase remains in the vessel, and "completely dispersed," where the liquid/liquid dispersion is distributed uniformly throughout the vessel. In a liquid/liquid system this can be quite difficult to detect [30].

However, the experiments here were carried out to determine the impeller speed where the "just dispersed" condition is achieved. Therefore, a small amount of petroleum oil was used, added on top of the continuous phase. The dispersed phase (phase fraction < 1%) was blended with a non-water soluble black and red dye (Sudan black and Sudan red). This increases the visibility of the point, where the lighter phase is drawn into the continuous phase as a function of the stirrer speed. The physical properties of the used dispersed phase are given in Table 1.

Table 2 – Listing of the data on used petroleum oil

γ [mN/m]	γ [mN/m] with dye	ρ_d [kg/m^3] at 20°C	η [mPa·s]	c_{dye} [g/L]
42	38.5	790	0.65	0.075

3.3 Numerical scheme

The computational fluid dynamics method, which solves the partial differential equations describing fluid flow, has proved to be a useful tool for fluid dynamics studies. The flow in stirred tanks is 3-dimensional, complex and due to the rotation of the impeller unsteady. In the area surrounding the impeller the flow is highly turbulent and swirling.

In this study, only the smallest vessel ($T_{1,A}$ = 155 mm) with the standard retreat curve impeller has been analyzed numerically. For the simulations the commercial CFD-package Star-CCM+ by CD-adapco was used. The simulations were carried out as a single phase system with the default values of water and k-ω turbulence model.

To reduce calculation time for a full 3-dimensional model, the Moving Reference Frame (MRF) in conjunction with steady state assumption was used. The reliability of the steady state assumption in combination with MRF was verified with a transient simulation where the mesh motion was explicitly performed. The simulation showed only low fluctuations of the

torque over the time. Therefore, the steady state assumption and MRF is suitable for these simulations. The simulated torque M on the stirrer and the shaft was used to determine the power consumption and the power number Ne of every simulated application.

$$Ne = \frac{2\pi M}{\rho n^2 D^5} = \frac{P}{\rho n^3 D^5} \tag{7}$$

In the simulations M was computed based on the forces acting on shaft and blades, while the other physical and process properties were specified as constant by the user (see Table 3).

Table 3 – Listing of the used physical and process properties

ρ [kg/m^3]	n [rpm]	T [mm]	D/T
997.63	410	155	0.6

All simulations were done on a polyhedrial grid. Five computational grids of different cell sizes were used in the numerical simulation to test the effect of the grid on the independency of the predicted torque and power consumption. The simulations were carried out for an H/T ratio equal to one, meaning a reactor volume equal to 2.6 L. The number of cells for this application was set to $9.3 \cdot 10^5$ (see Figure 3) and increased for increasing reactor volume. The turbulent power number obtained with different meshes are presented in Figure 3, which shows that the effect of the grid is negligible for $n_{cells} > 9 \cdot 10^5$. The computation was considered converged when the normalized residuals for each primary variable dropped well below 10^{-4}. Additionally, the used grid for the computational study is given in Figure 3.

The axial circulation volume flows are computed out of the simulation results following the continuity equation under the assumption of constant density. Two sections of the vessel are used as boundaries for the mass balance – one above and one below the impeller. Each section is separated into 1000 cells with approximately equal area A_i. The average axial velocity (z-component) w_i of each cell i is used for the calculation of the local volume flow. The summation of the local values represents the circulation volume flow.

$$\dot{V} = \sum_{i=1}^{1000} \dot{V}_i = \sum_{i=1}^{1000} w_i \cdot A_i \tag{8}$$

The mixing time is correlated to the circulation volume flow throughout the reactor and the corresponding circulation time:

$$\theta_{95} \propto t_c = \frac{V}{\dot{V}} \tag{9}$$

To quantify the hydrodynamics of the single phase flow in the reactor and to evaluate the quality of the CFD-simulations, particle image velocimetry (PIV) measurements were carried out.

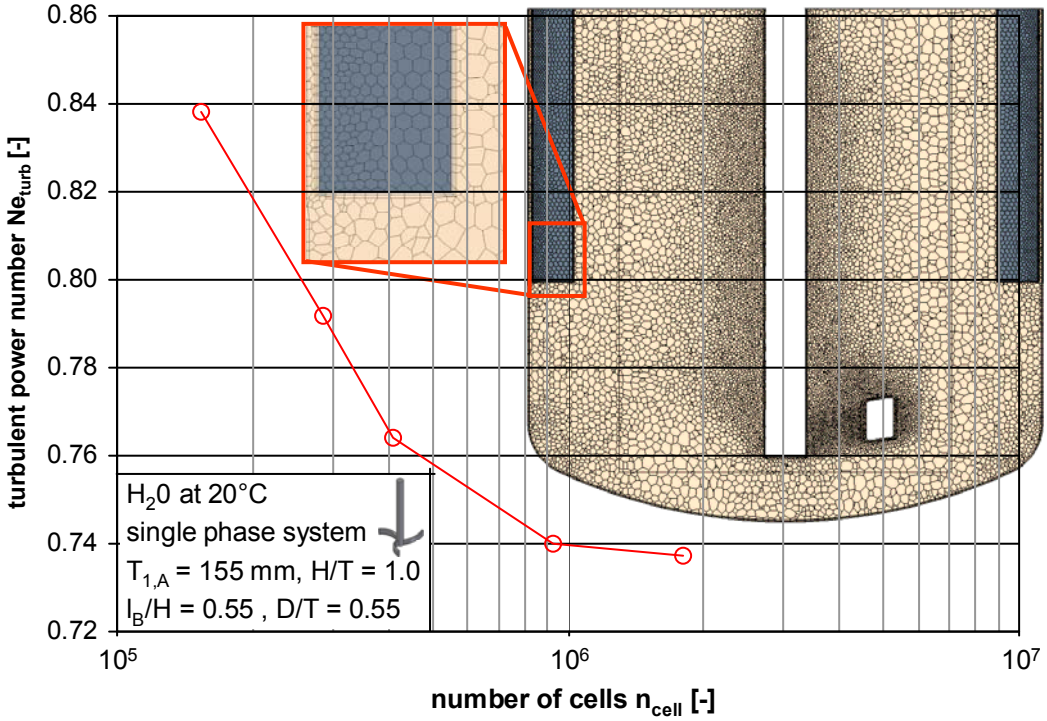

Figure 3 - Sensitivity analysis of predicted power numbers on number of cells used in the grid

4 RESULTS AND DISCUSSION

The decision process for the suitable mixing equipment is crucial for effective polymerization processes. The influence of baffles is one of the least investigated geometrical parameter for agitated reactors, especially for large aspect ratios. Therefore the first part of this chapter deals with extensive analysis of the baffling effect in slim reactors. Based on these results, an optimal impeller configuration for slim polymerization reactors is defined in the second part of this chapter.

4.1 Baffling effect

The immersion depth of baffles profoundly modifies the spatial distribution of the turbulent dissipation rate within a reactor. Since it also modifies the flow field, the residence time of a dispersed phase in the different zones of the reactor is affected. In a previous study the influence of the immersion depth of two baffles on the transient drop size distribution was studied [1]. Surprisingly, the Sauter mean diameters are clearly divided into two different regimes – under and above a certain baffle length l_B. The drop sizes for $l_B/H < 0.43$ are constant but two times larger than the constant drop size results for increasing $l_B/H > 0.43$. The influence of the baffling effect on power number, flow field and thereby the mixing time will be discussed in

this subchapter. These items are thought to be influential for optimal operation of a polymerization process.

4.1.1 Power number

The power number is a clear criterion for the energy consumption of a stirred system especially if the tip speed needs to be hold constant as desired in the presented project. The investigations have the aim to complete the power analysis which have already been carried out by the authors for slim reactors [1, 31]. The results of turbulent power numbers ($Re \geq 2.4 \cdot 10^4$) for different impeller systems as a function of the immersion depth of the baffles are presented in Figure 4.

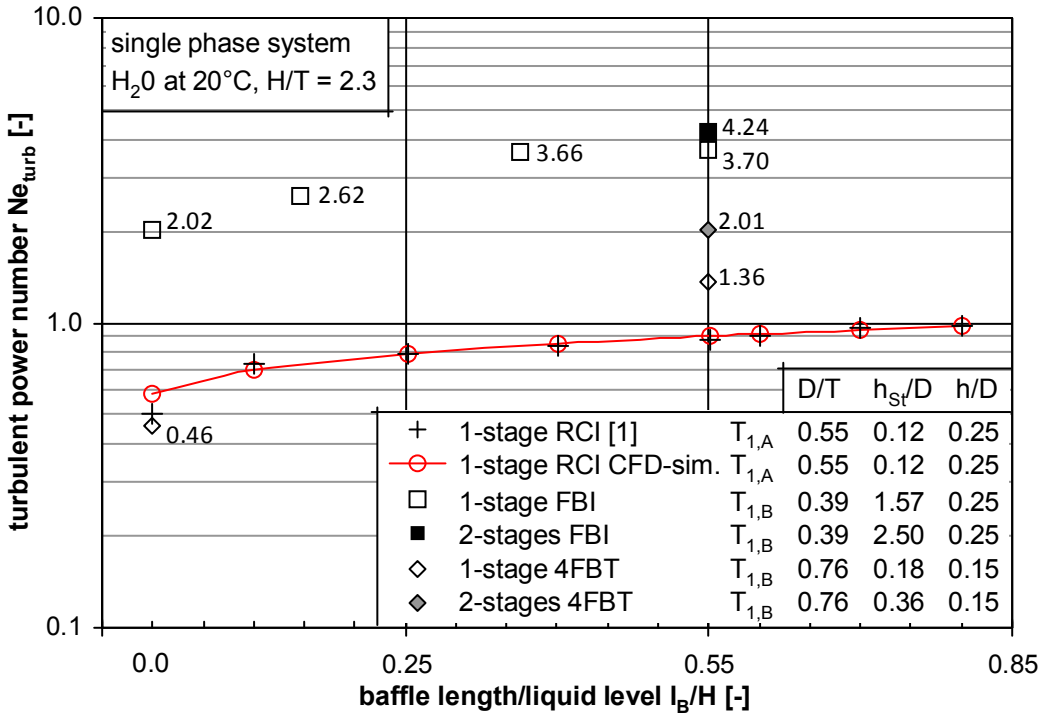

Figure 4 – Comparison of urbulent power numbers for different impellers from experiments and simulations

The development of the power number is shown for the RCI (cross symbols) and the single stage FBI (open squares). The power number of the single stage 4FBT are given for the unbaffled case and for $l_B/H = 0.55$. The general tendencies are the same for all investigated applications – with increasing baffle length, the torque and therefore the power numbers increase. Such results have been reported in literature for single Rushton turbines [32] as well as for dual Rushton turbines [33]. This physically expected behavior is excellent predicted by the CFD-simulations for the standard retreat curve impeller. Only the unbaffled case showed significant differences (around 13%). There, the simulations over predicted the torque. All simu-

lations were carried out as single phase simulations with a fixed surface. Multiphase simulations are highly computationally expensive because there are roughly twice as many equations to be solved as for a single phase simulation and the convergence is slowed due to the complexity of the multiphase physics [34]. The influences of the free surface and the development of a deep vortex are neglected in the simulations in this study. This leads to a higher torque for the unbaffled case than in reality.

The turbulent power numbers for the other impellers investigated (single and dual 4FBI, dual FBI) are also given in Figure 4. The results are in the same range as found by Jüsten et al. [35]. The difference may be explained in terms of the different stirrer diameter / vessel ratios. As this ratio is 40% larger as in this study also the power numbers are larger. The results of power consumption in Figure 4 provide a necessary foundation to determine efficient stirrer applications for slim reactors, useable for polymerization reactions.

4.1.2 Mixing time

In liquid-liquid systems, the resulting drop size distribution depends on the competing phenomena of drop breakage and drop coalescence. In stabilized emulsions, mainly used for polymerization reactions, drop breakage is the major phenomenon which determines the drop size distribution. While drop breakage occurs mainly in the stirrer region, the circulation loop within the reactor highly influences such liquid-liquid systems. The circulation flow in the reactor can be directly related to the mixing time with a correlation constant (equation (1)). CFD simulations have been used to determine the axial volume flow rates. These flow rate are than used in multi zonal population balances for more precise prediction of the drop sizes in such systems [1, 31]. The results of these numerical investigations are given in Figure 5. An exemplary 3 dimensional vector plot of the local velocities w_i in z-direction is embedded in Figure 5 for $l_B/H = 0.1$. Additionally the two mentioned intersection planes above and under the impeller are visualized. The calculation of the circulation flow rate is carried out according to equation (8). The arrows show the local streams always on the local planes A_i, leaving the impeller region. In the center of the vessel the flow direction is down through the impeller section. The direction changes with increasing distance from the center axis to a maximum value of the up flowing streams and decreases to zero at the reactor wall.

Although the drop size is constant at two different size levels under and above a certain baffle length [1], the predicted volume flow is continuously increasing for increasing baffle length. The tangential velocities are redirected by the baffles. This phenomenon is intensified by deeper immersions of the baffles. This leads to the conclusion, that the development of the axial volume flow with varying baffle length is not responsible for the drop size leap. To test this assumption, experimental mixing time measurements are carried out.

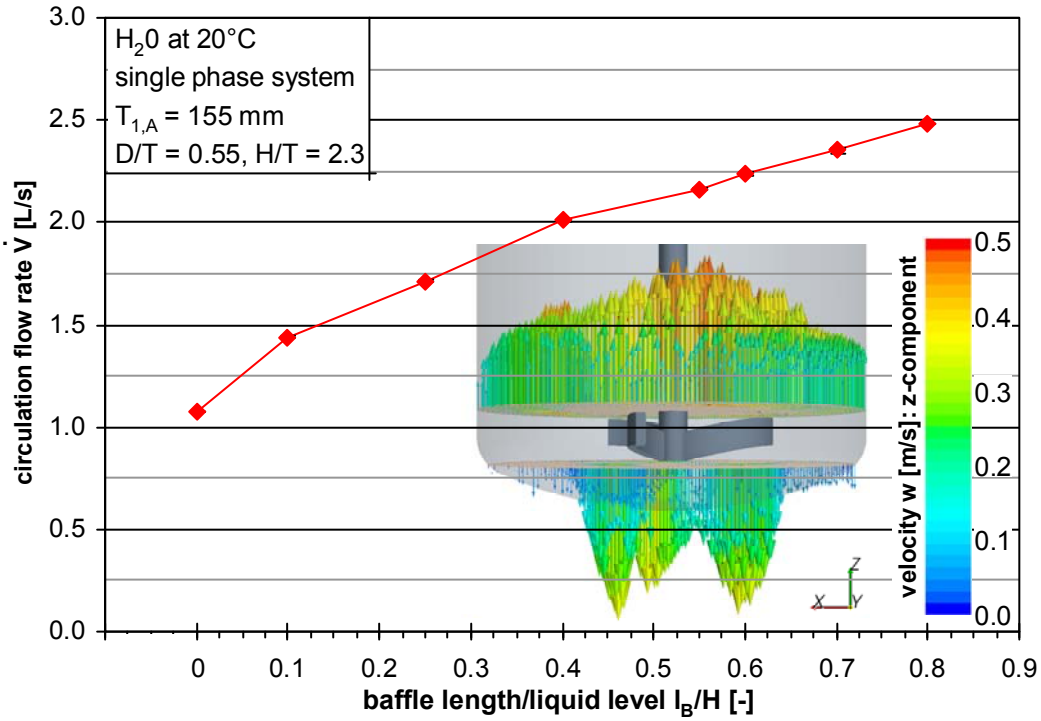

Figure 5 - Simulations of the axial volume stream as a function of the baffle length for the retreat curve impeller

The results of the dimensionless mixing time as a function of the baffle length for various impellers are given in Figure 6. The experimental results are compared with theoretical correlations (see equation (2)) and CFD-simulations. As well as the correlations, the simulations and the experimental data follow the same trend for all the different applications: An increase in baffle length leads to a decrease in the mixing time, if all other parameters are kept constant. This is very clear for the single stage flat blade impeller, the four bladed flat blade impeller and the retreat curve impeller with $h_{St}/D = 0.12$. The trend in the data from the RCI with double blade height is hard to determine. However, all other impellers are following the same trend. They show a decrease in mixing time with increasing baffle length and this means with increasing power input.

To evaluate the quantity of this influence, the proposed proportionality based on equation (2) is given for the FBI and the standard RCI (the two equations in Figure 6). The values have been calculated based on the experimentally achieved power number (see Figure 4 and [1]). All other dependencies ($5.2 \cdot (T/D)^2$) stay constant and are pulled together in the parameter C. Two major drawbacks exist. Firstly, the proportionality is much too weak for the flat blade impeller and slightly too weak for the RCI. Secondly, the absolute values achieved by equation (2) are too low by a factor of 8 for the FBI and by a factor of 6 for the RCI. This means that the used parameter C_{FBI} has to be 8 times larger to fit the unbaffled value than it has to be according to equation (2). The same is true for C_{RCI}, which has to be six times larger than pre-

dicted by equation (4). Both deviations may be caused by measurement errors occurring in the visual technique used to determine the mixing time. However, the huge deviation in the absolute values may be rather due to the fact that standard correlations used in literature are for aspect ratios around one. The trend of the predictions would be the same using equation (4), due to the same proportionality on the power number and no extra dependency on the baffle length in this correlation. With these results we affirm a careful analysis of the system and a careful use of the presented correlations in slim reactors.

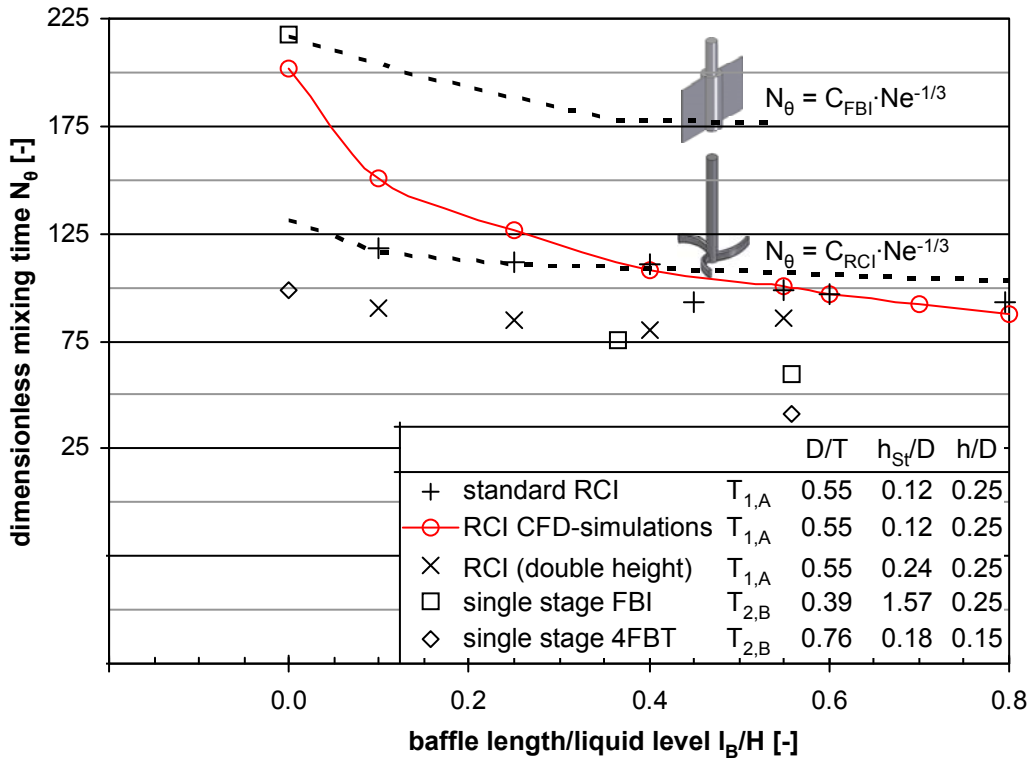

Figure 6 - Dimensionless mixing time as a function of the baffle length for various single stage impellers in a single phase system at H/T = 2.3

The mixing time from the CFD-simulation results is computed by using equation (9) and the results for the axial volume flow, presented in Figure 5. This calculation results in the circulation time for the reactor which has to be transformed into the mixing time. The circulation time multiplied by a factor of five is an excellent fit with the experimental mixing times and in agreements with the results of Nienow [17].The results for the lower immersion depth of the baffles are over predicted by the simulations.

All these experimental and theoretical results describe the influence of the baffle length meaningfully and allow deeper insights into the flow regime in slim reactors. However, these re-

sults are not able to explain the drop size leap at a certain point of l_B/H (around 0.43) reported by Maaß et al. [1].

4.1.3 Flow field

Stream lines are used in Figure 7 to illustrate and analyze the 3 dimensional flow field. For comparative purposes, all parameters of the stream lines are kept constant – space of origin, observed time and number of visualized stream lines. Figure 7 shows clearly the necessity of using baffles for agitated systems. A significant change in stream line behavior is shown by changing the system from unbaffled to baffled with $l_B/H = 0.1$. There are low axial velocity components in the unbaffled system, but instantaneously occur even with very low baffle lengths. The streamlines for l_B/H follow helicalcurves at the vessel wall to the surface and are pumped down at the impeller shaft in the middle of the reactor. The homogeneous, heli flow structure is disturbed and turns into a more random flow field by further increase of the baffle length. Inhomogeneities are created, the velocities are increased and thereby the tracked distances of every stream line in the observed interval.

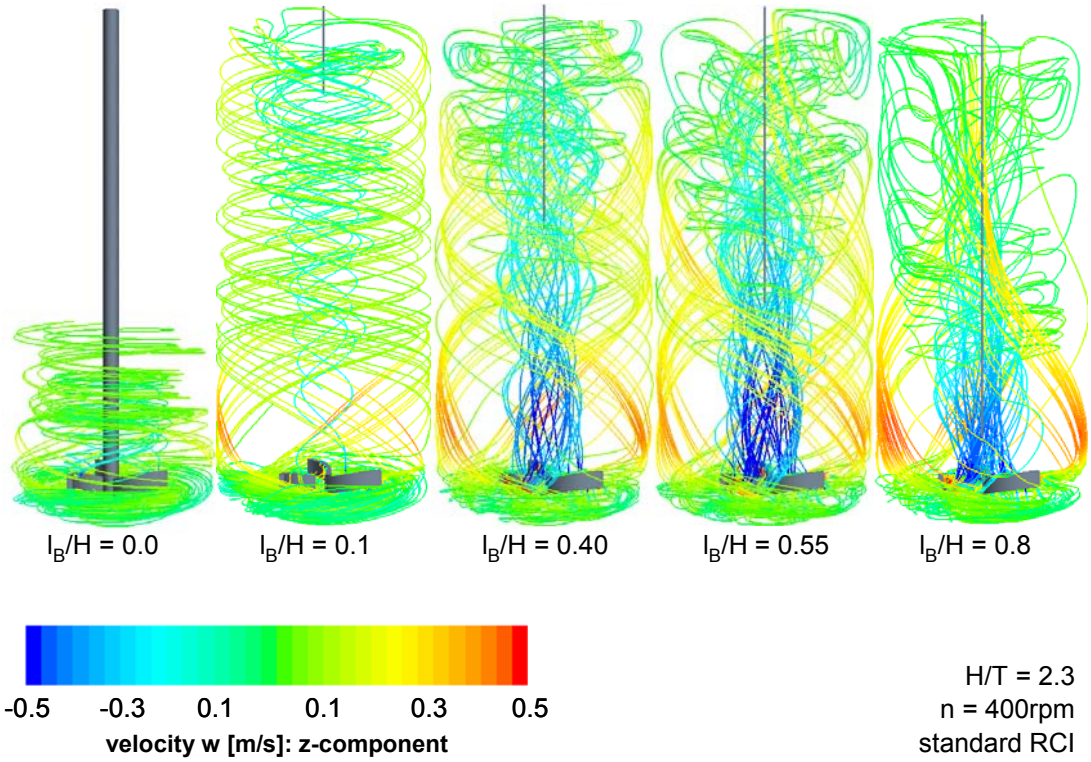

Figure 7 - Streamlines for unbaffled and baffled system with increasing baffle length l_B/H = 0.1 until 0.8

The CFD simulations were compared with PIV measurements, using a µPIV [36]. Simulations and experiments showed the same structure of the macroscopic flow. Since the flow was fully turbulent ($Re = 5 \cdot 10^4$ at the 400 rpm with $w_{tip} = 1.8$ m/s), this general flow pattern re-

peatedly measured for all investigated baffle lengths. Larger immersion depths of the baffles lead to stronger disturbances of the tangential circulations. The flow is more strongly redirected in axial direction.

Based on these experiments and simulations no significant differences of the 3 dimensional flow field are found at the drop size leap region [1], which is at the baffle lengths between $l_B/H = 0.4$ and 0.55,(see Figure 7). No clear reasons could be determined why this is the turning point of the drop sizes in the comparable liquid-liquid system. Velocities and even paths of the streamlines in the 3 dimensional flow fields are similar. Additionally, no strong influence on either the mixing time or the power number has been observed for this region in this and previous studies.

The immersion depth of the baffles was fixed at $l_B/H \approx 1.0$ – the fully baffled condition in the following investigations. This will provide extensive turbulences throughout the reactor and therewith minimize the mixing time.

4.2 Impeller configurations

4.2.1 Mixing time

The dimensionless mixing times in the turbulent regime over the Reynolds number is given in Figure 8. Four different impeller types are compared with each other. Additionally the cumulative stirrer height was increased for all 4 configurations (see the sketches of the agitation system used in Figure 8). This was done either by introducing a second agitation stage or, for the retreat curve impeller by doubling the single stage stirrer height. All other geometry parameters have been kept constant. All measured mixing times are almost constants over Reynolds number. This is in excellent agreement with the theory [20] and shows the reproducibility of the experimental work.

The 4FBT is the most efficient out of the single stage impellers. The lowest dimensionless mixing times are achieved ($N_\theta = 40$) with moderate power numbers (Ne = 1.36) for the 4FBT. On one hand, this supports already reported results from literature that large D/T ratios are highly efficient for mixing with single stage impellers [17]. On the other hand, the same result is achieved with the flat blade impeller. The highest power consumption (Ne = 3.70) delivers only moderate results for the dimensionless mixing time ($N_\theta = 60$). Therefore the FBI needs more power than the 4FBT and mixes worse.

The increase in stirrer height gives the same trend for the single stage RCI and for introducing a second agitator stage - with increasing h_{St}, N_θ is decreasing. The amount of decrease is not by far in the same range as the increase in the power consumption. The turbulent power number almost doubles by doubling the stirrer height for the RCI (1) and the CBI [31], while N_θ is only decreased by 10%. The same trend is found for the FBI and the 4FBT, although the 4-bladed flat blade turbine also shows the higher efficiency of a double stage impeller compared

to the other impeller configurations. Increases in power consumption by 50 percent generate a decrease in the mixing time by 25 percent.

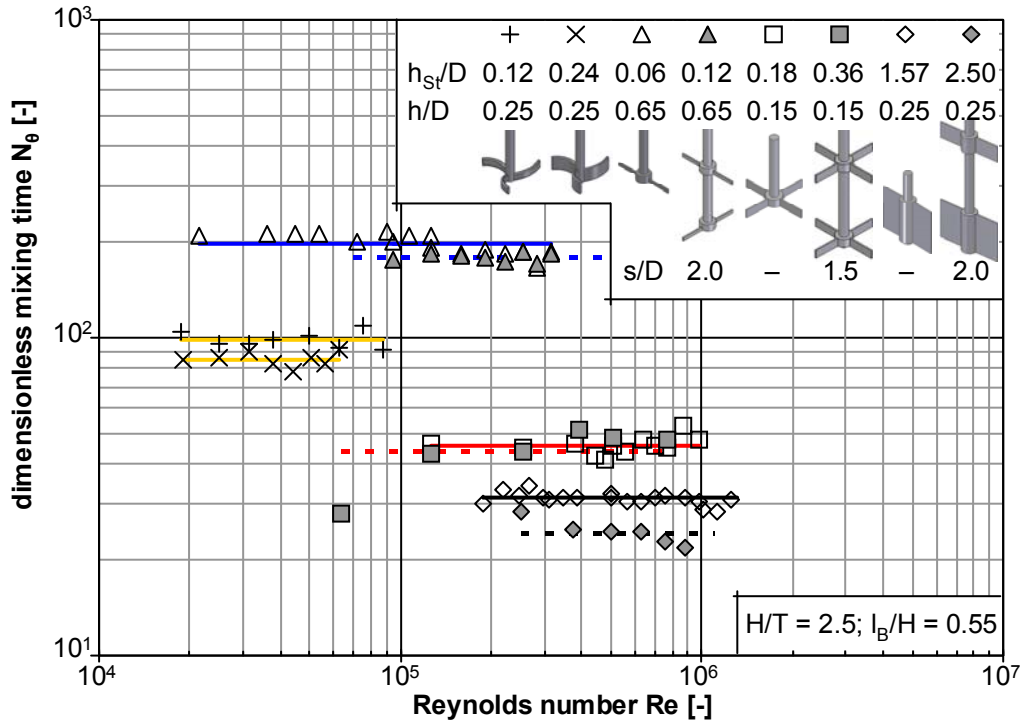

Figure 8 - Dimensionless mixing time over Reynolds number for different stirrer applications in slim reactors

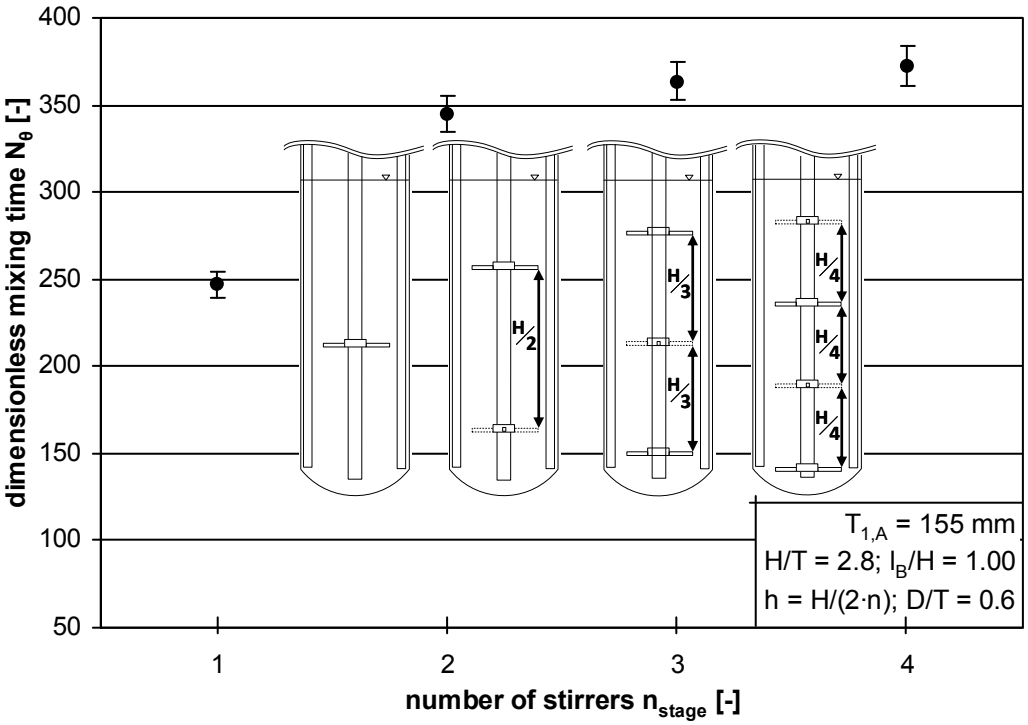

Figure 9 - Dimensionless mixing time for different number of stages with equal stirrer interspaces over the reactor height

Based on these results, the number of agitation stages was increased for the crossed blade impeller. The clearance between the agitation stages was always equally distributed over the vessel height (see Figure 9). The increase of the power number for this kind of stirrers is linear with the number of stages [31]. The power number increases from 0.41 to 1.17. Surprisingly the dimensionless mixing time also increases from 250 up to 375. The different agitator stages lead to compartments with a certain residence time for the fluid. Thereby the compartments act like a separation plane for the homogenization process. This barrier effect runs into a maximum for a constant vessel height. By introducing more agitation stages, the number of compartments in the reactor is increased. However, due to the constant reactor volume, the size of and thereby the residence time in the single compartment is decreased. The following Figure 10 shows how and where the separation plane is introduced into the system.

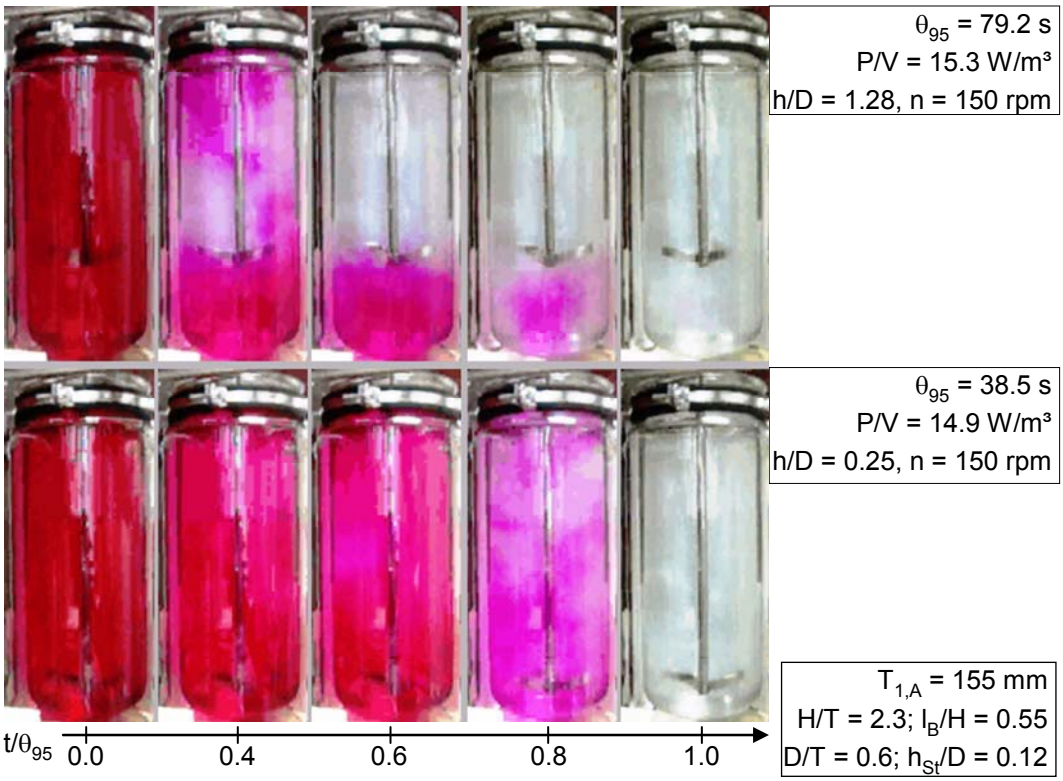

Figure 10 - Experimental decolorization of retreat curve impeller systems in dependency on stirrer bottom clearance and corresponding fluid flow compartmentalization

The strong influence of compartmentalization is shown in Figure 10 for the retreat curve impeller. Two image series represent two decolorization experiments for different stirrer bottom clearance. All other geometry parameters were kept constant. The higher installed impeller needs 10% more power and more than twice the time to achieve 95% degree of mixing. The space under the low hanging impeller is too small to build a loop and correspondingly a compartment. Therefore only one compartment has to be mixed. With enough space under the

impeller like in the first case in Figure 10, two compartments are built. The exchanges between the compartments seem to be poor. The mixing time for the upper compartment is the same as the one for the whole reactor with the low positioned impeller. After the first compartment is homogenized, the second compartment starts to decolorize. This behavior can not be predicted without the knowledge about the flow field. Only this knowledge delivers the number and the volume of compartments and thereby the number of barriers and an approximation of the mixing time.

For a constant reactor volume at H/T = 2.8, single, double, triple and quadruple crossed blade impeller configurations were tested (see Figure 11). The strong sensitivity of the dimensionless mixing time on the impeller constellation was analyzed. No clear tendency can be determined. The set-up with four agitation stages and a stirrer clearance s/D = 1 shows the highest mixing times, while the set-up with three impellers and again a stirrer clearance s/D = 1 shows the lowest mixing times. Two stages were pulled together from the quadruple impeller for a third constellation. This did not affect the power number (see Maaß et al. [31]).

The dimensionless mixing time was decreased by one third. This unification decreases the number of compartments from 4 to 2. The increased volume of each compartment has a lower influence on the axial mixing than the barrier effect of several compartments.

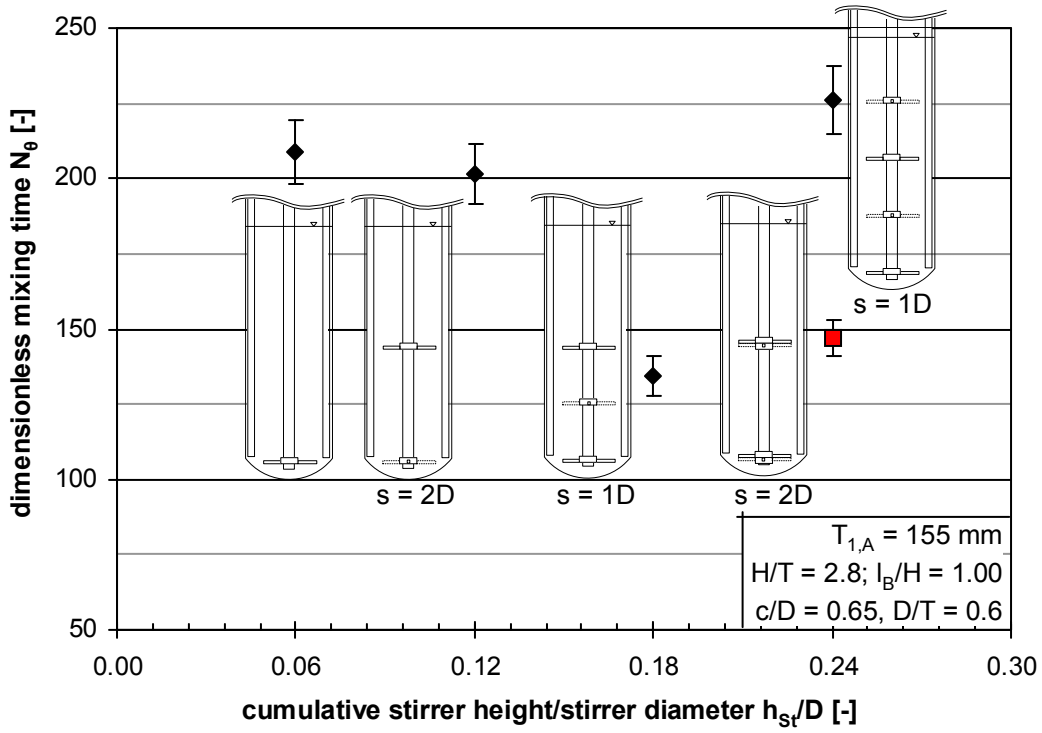

Figure 11 - Dimensionless mixing time for different number of stages

The single stage impeller is the most efficient mixer. This set-up homogenized the complete reactor in the same order of magnitudes as the other set-up despite having the lowest power number (0.36). Again, this behavior can not be predicted using classical correlations for the mixing time. A detailed flow field analysis would be necessary.

To quantify the dependency of the dimensionless mixing time on the stirrer-bottom and the stirrer-stirrer clearance, several investigations have been carried out with a varied dual crossed blade impeller set-up. At constant reactor volume, aspect ratio and baffle length, the distance between the two impellers was increased, starting with almost no distance (s/D = 0.06) as a single stage in the middle of the reactor liquid level and ending with s/D = 3 (see Figure 12 a-h). The eight reactor sketches are lined up in the same order as the data point over the abscissa.

The mixing time increases with increasing stirrer distance until a local maximum is reached for s/D = 1. Then N_θ decreases until the minimum of N_θ = 200 is reached at s/D = 2. After that distance, the dimensionless mixing time increases again. The maximum is reached at s/D = 3 with N_θ = 380.

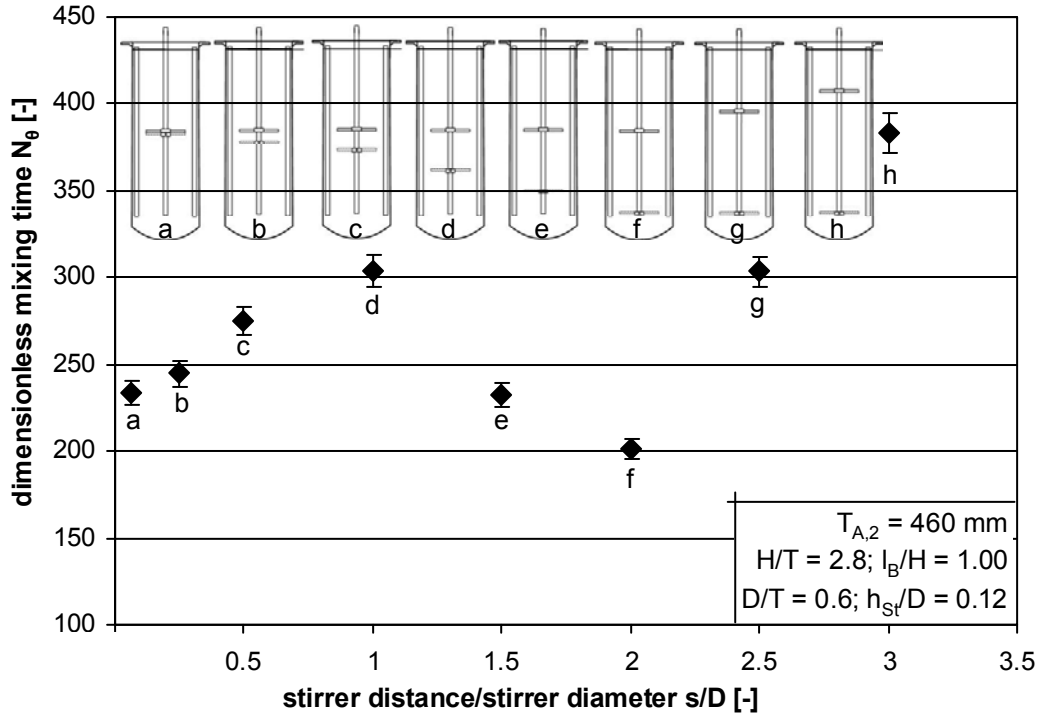

Figure 12 - Influence of stirrer distance of dual crossed blade impellers on dimensionless mixing time

The decolorization for s/D ≤ 1 shows (Figure 12 a-d) that the two impeller stages are working as one. Two loops are created, one above and one below the two agitators. If the stirrer distance is increased, a third (Figure 12 b & c) and even a fourth loop (Figure 12 d) are caused.

This increases the number of compartments and thereby the number of barrier stages in the reactor. The axial mixing is relatively poor. For $1.5 \leq s/D \leq 2.0$ the effect of the stirrer bottom clearance causes a decrease in the dimensionless mixing time (Figure 12 e & f). The lower clearance reduced the size of the loop under the impeller until no significant circulation loop could develop (see also the decolorization in Figure 10). This decreased the mixing time by reducing the number of separation planes and thereby increased the axial mixing. A further increase in the stirrer distance for more then twice the stirrer diameter (Figure 12 g & h) causes a more inhomogeneous concentration field. Fast decolorization is measured here for the highest part of the reactor between the surface and the highest impeller. Contrariwise the decolorization for the second loop under the upper impeller stage takes much longer than in all the other configurations. The axial mixing here shows the poorest results. This leads to the conclusion that radial impeller should be configured with $s/D = 2$, starting with one impeller close to the bottom of the reactor.

4.2.2 Minimum dispersion speed

Based on the mixing time results, some selected configurations were also tested for their ability to disperse a lighter phase into a heavier one. This is one of the major tasks for impellers in polymerization reactors. Especially slim reactors exhibit major challenges to completely introduce the dispersed phase from the surface into the vessel [31]. The dual and triple configurations with the fastest mixing (see Figure 11 and Figure 12) were tested against four different single stage impellers, which all obtained mixing times in the same range as the multiple stage systems.

The vessel height/vessel diameter ratio was increased for this investigation. The results are presented in Figure 13. All four single stage configurations show a significant increase in minimum dispersion speed with increasing aspect ratio. This increase is following an exponential trend. The influence of the stirrer bottom clearance was also investigated (see Figure 13 b and d). Both PBI had a stirrer height $h_{St}/D = 0.12$. The bottom clearance was increased from $h/D = 0.65$ to 2.65. This leads to an increase in the turbulent power number by 8 percent by decreasing the minimum dispersion speed by 25 %. This shows clearly the influence of the long distances from the surface to the impeller for low installed stirrers ($h/H < 1/3$). At a certain point of H/T, the low impellers will not be able to sufficiently disperse. The two multi stage impeller systems show no dependency of n_{min} on H/T for the range investigated (see Figure 13 e and f). The stirrer speed stays constant (around 125 rpm for e, around 100 rpm for f). For aspect ratios smaller than 2.5, it seems that multiple impellers are less efficient or as efficient as comparable single stage impellers with same power consumption. For $H/T > 2.5$ the multiple impeller configurations are much more efficient.

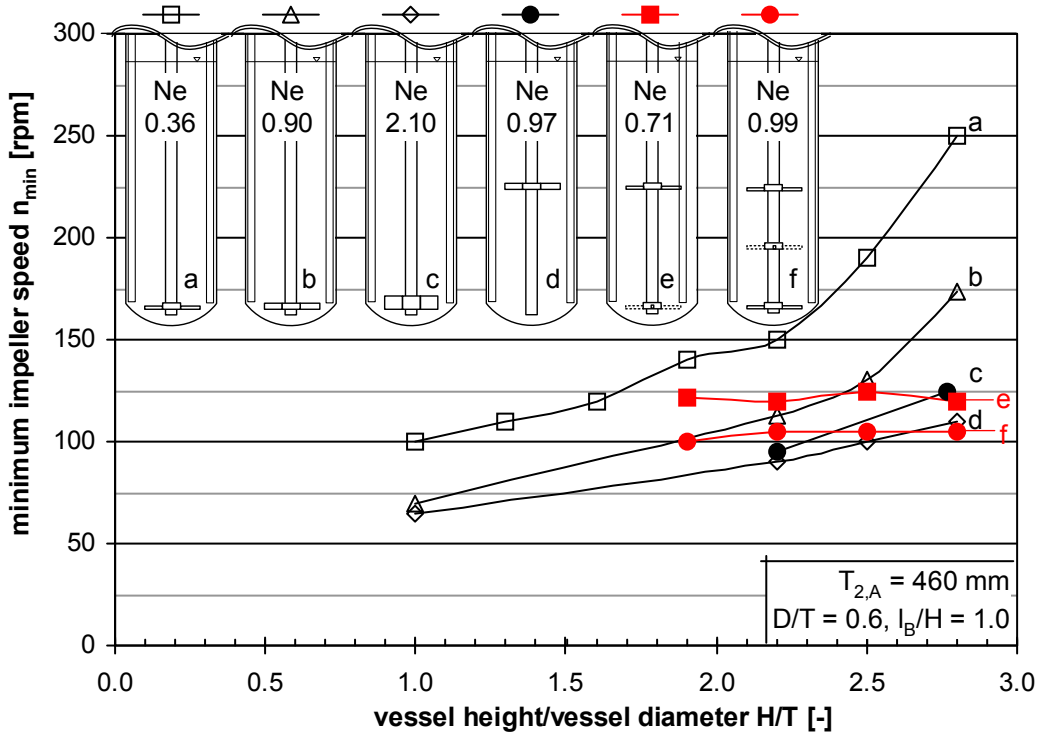

Figure 13 - Minimum dispersion speed for various single and multi stage crossed blade impeller configurations

The power analysis of the multiple impellers shows that the dual impeller system is more efficient. Although the minimum dispersion speed is almost 20 percent higher the power consumption is decreased by more than 30 percent.

This analysis shows the need for a broad analysis of the flow field in slim reactors, to be able to predict all needs in such vessels, like homogenization and dispersion.

5 SUMMARY AND CONCLUSION

In this study detailed experiments and simulations have been carried out for better understanding of slim reactors used for polymerization reactions. Two major tasks motivated this study. Firstly the determination of an optimum configuration for a multiple impeller application, based on its ability to disperse a lighter phase into a heavier phase and to fulfill fast mixing at minimal power consumption. Secondly the analyses of the influence of baffle lengths on single stage impellers in a slim reactor.

The analysis of the baffling effect is based on previous studies analyzing drop sizes in liquid-liquid systems. They have shown unpredictable drop size behavior at an immersion depth $l_B/H \approx 0.43$. This could not be explained in this study with the achieved results for the power consumption, mixing time and macroscopic flow field as a function of the baffle length. All characteristics, the experiments as the simulations, change monotone with increasing baffle

length opposed to the drop sizes reported by Maaß et al. [1]. A more detailed analysis with higher time and space resolution is necessary and is planed for the future work using CFD. So far, fully baffled liquid-liquid system is recommended to avoid the occurrence of unpredictable dispersion results.

Furthermore, the power consumption, mixing time and minimum dispersion speed are determined for five different stirrers under turbulent conditions. It is found that the dimensionless mixing time is highly sensitive to the configuration of the impellers, with almost no dependency on the turbulent power number. The mixing time correlations tested in this study need parameter adaptation to predict the experimentally determined values in reactors with high aspect ratios. The CFD simulations of the mixing time, carried out for one impeller type, were in excellent agreement with the experiments.

Summarizing all flow results achieved in this study an optimum impeller configuration is recommended: multi stage impellers should be used rather than single stage impellers. These impellers save power and allow complete dispersion also for reactors with aspect ratios larger than 3. The first impeller should be installed close to the reactor bottom. The optimum stirrer-stirrer clearance was determined with two times the stirrer diameter, which is equal to 1.2·T in this study.

SYMBOLS

A - area of a section [m^2]

b - baffle width [m]

c - concentration [g/L]

C_i - empirical constants [-]

D - stirrer diameter [m]

d_P - particle diameter [m]

h - bottom clearance [-]

h_{St} - stirrer height [m]

H - liquid level [m]

l_B - baffle length [m]

M - trorque [Nm]

n - stirrer speed [1/s]

n_{cells} - number of cells in the used mesh [-]

n_{stage} - number of agitation stages [-]

n_B - number of baffles [-]

P - power [W]

s - stirrer distance, stirrer clearance [m]

t - time [s]

T - tank diameter [m]

V - reactor volume [m^3]

$\dot{V}$ - volume stream [m^3/s]

w - velocity [m/s]

γ - interfacial tension [mN/m]

δ - relative deviation of the local concentration [mol/L]

ε - $P/(\rho V)$ - energy dissipation rate [W/kg]

η - dynamic viscosity [mPa·s]

ν - kinematic viscosity [m^2/s]

ρ - density [kg/m^3]

$\theta_{1-\delta}$ - mixing time of a certain deviation [s]

θ_{95} - mixing time [s]

DIMENSIONLESS NUMBERS

$N_\theta = n\theta_{95}$ - dimensionless mixing time

$Ne = P/ \rho n^3 D^5$ - power number

$Re = nD^2/ \nu$ - Reynolds number

ABBREVIATIONS

4FBT - 4 bladed flat blade turbine

CBI - crossed blade impeller

CFD - Computational fluid dynamics

FBI - flat blade impeller

LES - large eddy simulation

PBI - parallel blade impeller

PIV - particle image velocimetry

RCI - retreat curve impeller

ACKNOWLEDGEMENTS

The authors gratefully acknowledge the financial support of the Vinnolit GmbH and the fruitful discussion and comments by Dr. Johann Hiermeier from the Vinnolit GmbH.

Mr. Steve Paschke for providing the opportunity of and the support with the PIV measurements is gratefully acknowledged. Furthermore we like to thank Ms. Elodie Lutz and Mr. Sven Federowitz for performing the experiments and Mr. Georg Brösigke for the simulation work.

The fruitful and valuable comments and remarks from the reviewers are gratefully acknowledged.

LITERATURE

[1] S. Maaß, F. Metz, T. Rehm and M. Kraume, Prediction of drop sizes for liquid-liquid systems in stirred slim reactors-Part I: Single stage impellers. Chem. Eng. J., 162 (2010) 792-801.
[2] G. Delaplace, L. Bouvier, A. Moreau, R. Guerin and J.C. Leuliet, Determination of mixing time by colourimetric diagnosis - Application to a new mixing system. Exp. Fluids, 36 (2004) 437-443.
[3] R. Mann, S.K. Pillai, A.M. Elhamouz, P. Ying, A. Togatorop and R.B. Edwards, Computational Fluid Mixing for Stirred Vessels - Progress from Seeing to Believing. Chem. Eng. J. Biochem. Eng. J., 59 (1995) 39-50.
[4] O. Visuri, M. Laakkonen and J. Aittamaa, A digital imaging technique for the analysis of local inhomogeneities from agitated vessels. Chem. Eng. Technol., 30 (2007) 1692-1699.
[5] N. Otomo, W. Bujalski, A.W. Nienow and K. Takahashi, A novel measurement technique for mixing time in an aerated stirred vessel. J. Chem. Eng. Jpn., 36 (2003) 66-74.
[6] W.M. Lu, H.Z. Wu and M.Y. Ju, Effects of baffle design on the liquid mixing in an aerated stirred tank with standard Rushton turbine impellers. Chem. Eng. Sci., 52 (1997) 3843-3851.
[7] E.A. Fox and V.E. Gex, Single-Phase Blending of Liquids. AIChE J., 2 (1956) 539-544.
[8] T. Moucha, V. Linek, K. Erokhin, J.F. Rejl and M. Fujasova, Improved power and mass transfer correlations for design and scale-up of multi-impeller gas-liquid contactors. Chem. Eng. Sci., 64 (2009) 598-604.
[9] Q. Zhang, Y. Yong, Z.-S. Mao, C. Yang and C. Zhao, Experimental determination and numerical simulation of mixing time in a gas-liquid stirred tank. Chem. Eng. Sci., 64 (2009) 2926-2933.
[10] M. Jahoda and V. Machon, Homogenization of Liquids in Tanks Stirred by Multiple Impellers. Chem. Eng. Technol., 17 (1994) 95-101.
[11] M. Jahoda, M. Mostek, A. Kukukova and V. Machon, Cfd modelling of liquid homogenization in stirred tanks with one and two impellers using large eddy simulation. Chem. Eng. Res. Des., 85 (2007) 616-625.
[12] A. Kukukova, M. Mostek, M. Jahoda and V. Machon, CFD prediction of flow and homogenization in a stirred vessel: Part I vessel with one and two impellers. Chem. Eng. Technol., 28 (2005) 1125-1133.
[13] M. Mostek, A. Kukukova, M. Jahoda and V. Machon, CFD prediction of flow and homogenization in a stirred vessel: Part II vessel with three and four impellers. Chem. Eng. Technol., 28 (2005) 1134-1143.

[14] Z. Jaworski, W. Bujalski, N. Otomo and A.W. Nienow, CFD study of homogenization with dual Rushton turbines - Comparison with experimental results part I: Initial studies. Chem. Eng. Res. Des., 78 (2000) 327-333.
[15] R.R. Hemrajani and G.B. Tatterson. Mechanically Stirred Vessels, in Handbook of Industrial Mixing: Science and Practice, E.L. Paul, V.A. Atiemo-Obeng, and S.M. Kresta, Editors. John Wiley & Sons, Inc.: Hoboken, New Jersey. 2004, pp. 345-390.
[16] S. Kresta and R.S. Brodkey. Turbulence in Mixing Applications, in Handbook of Industrial Mixing: Science and Practice, E.L. Paul, V.A. Atiemo-Obeng, and S.M. Kresta, Editors. John Wiley & Sons, Inc.: Hoboken, New Jersey. 2004, pp. 19-87.
[17] A.W. Nienow, On impeller circulation and mixing effectiveness in the turbulent flow regime. Chem. Eng. Sci., 52 (1997) 2557-2565.
[18] S. Corrsin, The Isotropic Turbulent Mixer: Part II - Arbitrary Schmidt Number. AIChE J., 10 (1964) 870-877.
[19] K. Rao and J.B. Joshi, Liquid-Phase Mixing in Mechanically Agitated Vessels. Chem. Eng. Commun., 74 (1988) 1-25.
[20] R.K. Grenville and A.W. Nienow. Blending of Miscible Liquids, in Handbook of Industrial Mixing: Science and Practice, E.L. Paul, V.A. Atiemo-Obeng, and S.M. Kresta, Editors. John Wiley & Sons, Inc.: Hoboken, New Jersey. 2004, pp. 506-542.
[21] J.B. Fasano and W.R. Penney, Avoid Blending Mix-Ups. Chem. Eng. Prog., 87 (1991) 56-63.
[22] A. Ochieng, M. Onyango and K. Kiriamiti, Experimental measurement and computational fluid dynamics simulation of mixing in a stirred tank: a review. S. Afr. J. Sci., 105 (2009) 421-426.
[23] S.S. Alves, J.M.T. Vasconcelos and J. Barata, Alternative Compartment Models of Mixing in Tall Tanks Agitated by Multi-Rushton Turbines. Chem. Eng. Res. Des., 75 (1997) 334-338.
[24] G.R. Kasat and A.B. Pandit, Mixing Time Studies in Multiple Impeller Agitated Reactors. Can. J. Chem. Eng., 82 (2004) 892-904.
[25] G. Ascanio, B. Castro and E. Galindo, Measurement of power consumption in stirred vessels - A review. Chem. Eng. Res. Des., 82 (2004) 1282-1290.
[26] J.W. Hiby, Definition and measurement of the degree of mixing in liquid mixtures. Int. Chem. Eng., 21 (1981) 197-204.
[27] M. Kraume, Mixing time in stirred suspension. Chem. Eng. Technol., 15 (1992) 313-318.
[28] A.H.P. Skelland and R. Seksaria, Minimum Impeller Speeds for Liquid-Liquid Dispersion in Baffled Vessels. Ind. Eng. Chem. Process Des. Dev., 17 (1978) 56-61.
[29] M.F. Kemmere, J. Meuldijk, A.A.H. Drinkenburg and A.L. German, Emulsification in batch emulsion polymerization. J. Appl. Polym. Sci. , 74 (1999) 3225-3241.
[30] D.A.R. Brown, P.N. Jones and J.C. Middelton. Experimental Methods - Part A: Measuring Tools and Techniques for Mixing and Flow Visualization Studies, in Handbook of Industrial Mixing: Science and Practice, E.L. Paul, V.A. Atiemo-Obeng, and S.M. Kresta, Editors. John Wiley & Sons, Inc.: Hoboken, New Jersey. 2004, pp. 145-202.
[31] S. Maaß, T. Rehm and M. Kraume, Prediction of drop sizes for liquid/liquid systems in stirred slim reactors - Part II: Multiple stage impellers. Chem. Eng. J., 168 (2011) 827–838.
[32] J. Karcz and M. Major, An effect of a baffle length on the power consumption in an agitated vessel. Chem. Eng. Process., 37 (1998) 249-256.
[33] J. Markopoulos, E. Babalona and E. Tsiliopoulou, Power consumption in agitated vessels with dual Rushton turbines: Baffle length and impeller spacing effects. Chem. Eng. Technol., 27 (2004) 1212-1215.
[34] J.P. Torré, D.F. Fletcher, T. Lasuye and C. Xuereb, Transient hydrodynamics and free surface capture of an under-baffled stirred tank during stopping. Chem. Eng. Res. Des., 85 (2007) 626-636.
[35] P. Jüsten, G.C. Paul, A.W. Nienow and C.R. Thomas, A mathematical model for agitation-induced fragmentation of Penicillium chrysogenum. Bioprocess Eng., 18 (1998) 7-16.

[36] S. Paschke, J.U. Repke and G. Wozny, Untersuchungen von Filmströmungen mittels eines neuartigen Micro Particle Image Velocimetry Messverfahrens. Chem. Ing. Tech., 80 (2008) 1477-1485 (in German).